Searching for evidence of interaction between the Of star HD 229196 and the interstellar medium

S. Pineault,[1][*] E. M. Arnal,[2,3] C. Cappa,[2,3] S. Cichowolski,[1,4] M. Normandeau[5] and N. St-Louis[6]

[1]*Département de physique et Observatoire du Mont Mégantic, Université Laval, Québec (Qué), Canada G1K 7P4*
[2]*Instituto Argentino de Radioastronomía, CC 5, 1894 Villa Elisa, Argentina*
[3]*Facultad de Ciencias Astronómicas y Geofísicas, Universidad Nacional de La Plata, Paseo del Bosque s/n, 1900 La Plata, Argentina*
[4]*Instituto de Astronomía y Física del Espacio (IAFE), CC 67, Suc. 28, 1428 Buenos Aires, Argentina*
[5]*Physics Department, University of New Brunswick, Fredericton NB, Canada E3B 5A3*
[6]*Département de physique et Observatoire du Mont Mégantic, Université de Montréal, Montréal (Qué), Canada H3C 3J7*

ABSTRACT

Massive stars with strong stellar winds are expected to have a huge impact on their interstellar surroundings, an effect which, in a surprisingly large number of cases, is not observed. This work is part of a concerted effort to obtain a better and more homogeneous observational data base with which to test the predictions of theoretical models. Analysis of the interstellar medium around the Of star HD 229196 shows that it coincides (in projection) with a region of lower radio continuum emission. This suggests that the star has shaped the surrounding interstellar medium via its ionizing flux and stellar wind. However, we find no clear evidence of the star's action in atomic hydrogen images. The radio continuum morphology and absence of a clear expanding H I shell are consistent with the possibility that the star, which is travelling supersonically at $\sim$30 km s^{-1} with respect to its local interstellar medium, is creating a weak bow shock. We cannot however rule out the possibility that the observed asymmetry is due to an inhomogeneous interstellar density distribution. We use data from the Canadian Galactic Plane Survey to carry out this study.

Key words: stars: individual: HD 229196 – stars: mass-loss – stars: winds, outflows – ISM: bubbles – ISM: structure.

1 INTRODUCTION

Massive stars have large ionizing luminosities, mass-loss rates ($\dot{M}$) and wind terminal velocities (v_{∞}) which generally affect the interstellar medium (ISM) on significant scales. A number of models have been developed to describe this interaction (e.g. Avedisova 1972; Castor, McCray & Weaver 1975; Weaver et al. 1977). The resulting structures are expected to take the form of a low-density, high-temperature cavity, known as an interstellar bubble, surrounded by an expanding envelope which, after it has cooled, may be seen as an expanding H I shell. If the star is either at rest or has a low spatial velocity with respect to its local ISM, and if this surrounding gas is reasonably homogeneous, it should be seen projected on to or close to the centre of a region of low H I emissivity (or H I minimum, for short). If however the star possesses a relatively large spatial velocity, one expects that a structure distorted along the direction of motion would form, either an asy-

metrical bubble (Weaver et al. 1977) or a bow shock, if the velocity is supersonic (Wilkin 1996). It is also possible that no conspicuous structures are formed if, for example, the surrounding ISM is highly inhomogeneous.

Observationally, the environments of the stars known to have some of the largest $\dot{M}$ (i.e. Wolf–Rayet, WR, stars) have been searched for bubbles. Many of these have been studied in detail in the optical (e.g. Chu, Treffers & Kwitter 1983; Lozinskaya 1992, and references therein), in the radio at modest (Arnal 1992; Cichowolski & Arnal 2004) and high (Cappa et al. 1996; Cazzolato & Pineault 2000; Cichowolski et al. 2001; Cappa, Goss & Pineault 2002a; Cappa, Goss & van der Hucht 2004, and references therein) resolution, and in the infrared (IR) (see Marston 1996, for a review). Not surprisingly, the agreement between observations and the models is highly variable. The WR 130 case (Cichowolski et al. 2001) is probably the best example of a classical bubble, with a conspicuous quasi-spherical cavity surrounded by a shell seen in the continuum, at radio and IR wavelengths, as well as in the 21-cm line of H I. Many stars however seem to have an associated and sometimes fairly regular H I shell, yet are missing a continuum

[*]E-mail: pineault@phy.ulaval.ca

counterpart, WR 143 being a representative case (Cazzolato & Pineault 2000). Furthermore, this star is located well off the centre of the H I structure, as also observed for many stars (Arnal 1992). A totally different situation is exemplified by WR 124 (Cichowolski et al. 2008), where the stellar spatial velocity is so high ($\sim$200 km s^{-1}) that it is the single most important parameter in determining the shape of the associated ISM structure, in this case, a bow shock.

In many cases, the large dimensions of the structures together with their low expansion velocities suggest that the massive progenitor (an O-type star) of the current WR star must also be responsible for shaping the bubbles. Consequently O- and Of-type stars are promising candidates to investigate the effects of stellar winds on the surrounding gas (Lozinskaya 1982, 1992). Indeed, several H I voids and shells have been found around massive O stars (Cappa & Herbstmeier 2000; Cappa et al. 2002b, 2003; Cichowolski et al. 2003). As observed for WR stars, the morphology of the H I structures is extremely diverse. For example, both BD+24°3866 and BD+24°3881 are Of stars considered to be members of the same Vul OB1 association (Garmany & Stencel 1992) at $l \sim 61°, b \sim 0°$ and a distance of 2.5 kpc. Yet the former is found located close to the inner border of a slowly expanding H I shell, whereas the same data show no conspicuous feature associated with the latter (Cappa et al. 2002b). In the case of HD 10125 (Cichowolski et al. 2003), an O9.7II star (Walborn 1971) located at a distance of 3 kpc and at $l \sim 128°$, $b \sim 1°.8$, where one expects confusion to be minimal, only weak evidence is found for a minimum in the H I distribution and a partial arc-like structure is seen in both H I and the radio continuum.

However, since the angular resolution in these prior studies varies from 1 up to 30 arcmin, it is difficult to compare their results meaningfully. As a matter of fact, there is a dearth of studies of the atomic hydrogen at angular resolutions that allow probing down to parsec scales. Given that atomic hydrogen is the most abundant and pervasive constituent of our galaxy and that massive stars, while rare, are the main source of energy that sculpts the Galaxy and impacts its evolution, looking at the coupling between the atomic hydrogen and massive stars is a crucial piece of the Galactic puzzle.

In order to minimize the impact of selection effects upon the deduced physical characteristics of ISM structures seen around massive stars, and therefore upon the deduced parameters of the winds creating them, it is highly desirable to use a homogeneous observational data base. The *Infrared Astronomical Satellite* (*IRAS*) observations provide such a data base in the IR at arcminute resolution. In the radio, the Canadian Galactic Plane Survey (CGPS; Taylor et al. 2003) now provides an equivalent data set. It is a high-resolution ($\sim$1 arcmin) H I line and 408- and 1420-MHz radio continuum survey of the Galactic plane obtained with the Synthesis Telescope (Landecker et al. 2000) of the Dominion Radio Astrophysical Observatory (DRAO). It provides a unique opportunity to carry out an unbiased homogeneous study of the ISM structures associated with massive stars and their evolved descendants, down to parsec scales, while avoiding preconceived notions about what the ISM around massive stars should look like. Since high-mass stars considerably stir up their surrounding ISM and are often found in complex regions, it is reasonable to expect some discrepancy between the well-behaved uniform density medium of basic stellar wind bubble models and the typical environment of massive stars.

The present authors have undertaken a project aimed at systematically studying the immediate vicinity of a number of stars expected to be major contributors in shaping the ISM including, in particular, Of stars. From an observational point of view it is a well-known

Table 1. Parameters of HD 229196.

Parameter	Value	References
Spectral type	O6III(n)(f)	4
Distance (kpc)	1.3	This paper
v_r (km s^{-1})	-38 ± 5	5
μ_α (mas yr^{-1})	-4.55 ± 0.72	*Hipparcos*
μ_δ (mas yr^{-1})	-4.54 ± 0.77	*Hipparcos*
μ_α (mas yr^{-1})	-2.2 ± 1.0	Tycho-2
μ_δ (mas yr^{-1})	-5.7 ± 1.0	Tycho-2
$\dot{M}$ (M$_\odot$ yr^{-1})	$<5.5 \times 10^{-6}$	1
	2×10^{-6}	3
v_∞ (km s^{-1})	2500	2
L_w (erg s^{-1})	3.1×10^{36}	2

References: (1) Bieging et al. (1989); (2) based on Howarth & Prinja (1989); (3) Lamers & Leitherer (1993); (4) Walborn (1973); (5) Wilson (1953).

fact that attempting to study the H I distribution towards a low Galactic latitude object is a very difficult task, for confusion effects arising from unrelated Galactic H I emission are important. Bearing this point in mind, we have mostly selected Of stars with relatively high Galactic latitudes. From the Galactic O-star Catalogue of Maíz-Apellániz et al. (2004), it is found that 32 Of stars fall within the sky area covered by the CGPS, and that only 13 have Galactic latitudes above $|b| \sim 1°.5$, including the Of star HD 229196. Its relative proximity to the Sun implies that any associated structure is expected to have a large and easily recognizable signature. Furthermore its large proper motion, together with its small distance, make it a particularly good prospect for investigating the possible effects of the stellar motion on the shape of any associated ISM structure.

HD 229196 is a giant of spectral type O6III(n)(f) (Walborn 1973), located in the Cygnus region at a Galactic longitude of 78°.76 and latitude of +2°.07. According to Maíz-Apellániz et al. (2004), it has a visual magnitude $V = 8.52$ and colour $B - V = 0.90$. Adopting $(B - V)_0 = -0.32$ (Schmidt-Kaler 1982) and $M_v = -5.78$ (Vacca, Garmany & Shull 1996), and using an extinction ratio $R = 3.1$, places this star at a distance of 1.3 kpc. For its proper motion, the *Hipparcos* and Tycho-2 catalogues give (μ_α, μ_δ) (mas yr^{-1}) = $(-4.55 \pm 0.72, -4.54 \pm 0.77)$ and $(-2.2 \pm 1.0, -5.7 \pm 1.0)$, respectively. Wilson (1953) measured a heliocentric velocity of -38 ± 5 km s^{-1} for this star.

Based on 5-GHz radio continuum observations, Bieging, Abbott & Churchwell (1989) found an upper limit, uncorrected for clumping, to the star's mass-loss rate of 5.5×10^{-6} M$_\odot$ yr^{-1}. The empirical relation obtained by Lamers & Leitherer (1993) yields a value of $\dot{M} = 2 \times 10^{-6}$ M$_\odot$ yr^{-1}. From the relationships derived by Howarth & Prinja (1989), the wind luminosity is 3.1×10^{36} erg s^{-1} (with a mass-loss rate of 5.5×10^{-6} M$_\odot$ yr^{-1}) and the terminal velocity $v_\infty = 2500$ km s^{-1}. The basic parameters and properties of HD 229196 are summarized in Table 1.

2 OBSERVATIONAL DATA

The radio observations presented here, of arcminute resolution in both the continuum and the 21-cm line of H I, are taken from the CGPS. Before assembly into a mosaic, the data for the individual fields are carefully processed to remove artefacts and to obtain the highest possible dynamic range, using the routines described by Willis (1999). Accurate representation of all structures to the largest scales is assured by incorporating data from large single antennae with data from the Synthesis Telescope, after
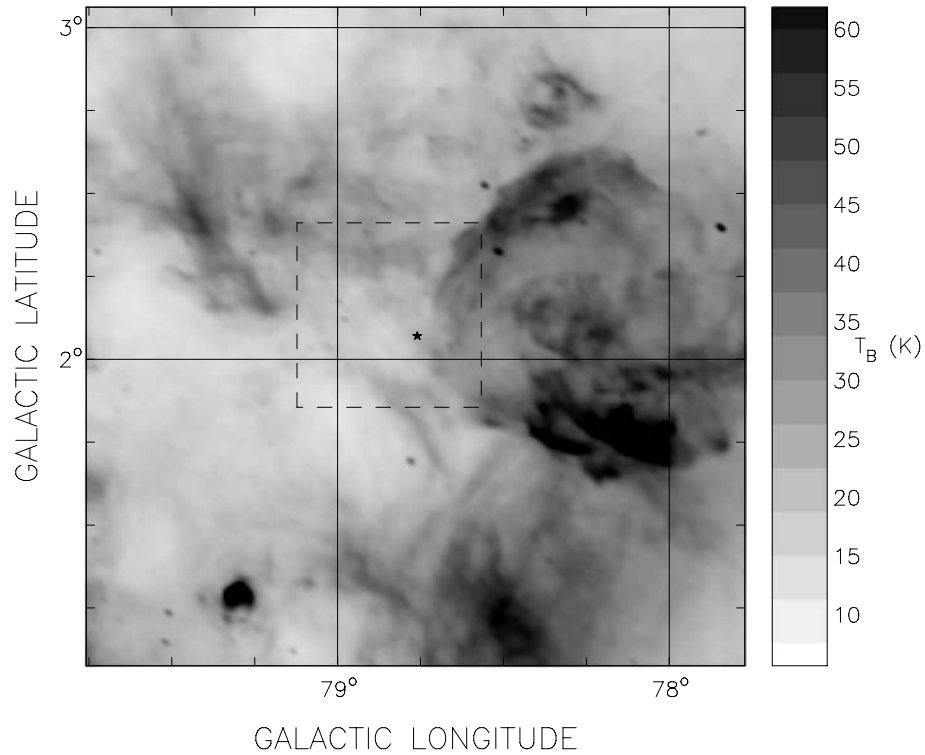
Figure 1. CGPS 1420-MHz continuum image centred on HD 229196 (position indicated by an asterisk). Resolution is 0.9×1.4 arcmin^2 (east–west $\times$ north–south in equatorial coordinates). Brightness temperature varies between 7.5 and 60 K. The dashed-line box outlines an area shown enlarged in Fig. 3.
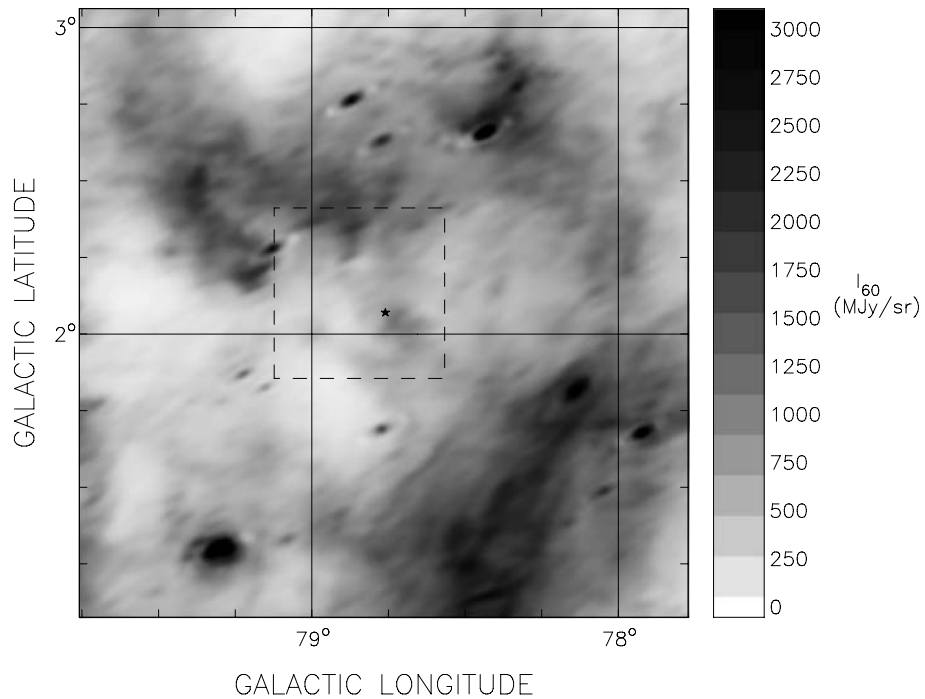
Figure 2. HIRES 60-μm emission. Resolution (slightly variable over image) is 1.7×1.0 arcmin^2 at a position angle of $31°$ (measured counterclockwise from the horizontal axis). Brightness varies between 50 and 3000 MJy sr^{-1}. The dashed-line box outlines an area shown enlarged in Fig. 3.

suitable filtering in the Fourier domain. Continuum data are derived from the 1.4-GHz Effelsberg survey (Reich, Reich & Fürst 1997). Single antenna H I data are obtained from a survey of the CGPS region made with the DRAO 26-m telescope (Higgs & Tapping 2000). H I data have a velocity resolution of 1.3 km s^{-1} with a channel separation of 0.82 km s^{-1}. The rms noise in the images at full resolution is 0.03 K T_B in the continuum and 3 K T_B in H I.

3 RESULTS

3.1 Radio, infrared and optical continuum

In order to appreciate the large-scale environment of HD 229196, we first show in Fig. 1(a) 1420 MHz radio continuum image of a large region in Cygnus covering an area of $\sim 2° \times 2°$. The dominant large nearly circular feature on the western half of the radio image (from here-on, all directions are with respect to Galactic longitude and latitude) is the well-known supernova remnant (SNR) G78.2+2.1 (e.g. Landecker, Roger & Higgs 1980; Zhang et al. 1997, and references therein). On the basis of H I absorption of the brightest continuum structures, Landecker et al. (1980) estimated its distance as 1.5 kpc. The remnant G78.2+2.1 will not be discussed further here as it is the subject of a current independent study (Ladouceur & Pineault, in preparation). The position of HD 229196 is indicated by an asterisk.

An inspection of Fig. 1 shows that the star appears projected within a region of moderately depressed radio continuum emissivity (centred near $l \approx 78°\,50'$, $b \approx 2°\,5'$ and about 18 arcmin in diameter) which could have been produced by the clearing action of the star's wind and ionizing luminosity. The asymmetry of the structure, in particular the non-central position of the star, could be due to the existence of a density gradient in this region and/or to the relative motion of the star with respect to its local ISM.

Fig. 2 shows the *IRAS* 60-μm image of the same field of view. The IR observations are the high-resolution-processed (HIRES) (Fowler & Aumann 1994; Cao et al. 1997) *IRAS* images produced at the Infrared Processing and Analysis Center (IPAC).[1] The image is the result of 20 iterations of the algorithm, giving an approximate resolution of 0.5 arcmin. This image appears at first sight drastically different from the radio image; however, except for the striking absence of the SNR in this band, most other radio features have IR counterparts. The cavity corresponding to HD 229196 seen in the radio continuum is also present, although it differs somewhat in detailed structure and is less clearly defined.

Fig. 3 is a close-up view showing the same small field in the radio continuum at 1420 MHz (top), 60 μm (middle) and in the optical (bottom; this figure is a red image extracted from the Digitized Sky Surveys[2]). The radio image shows more clearly the area of reduced emission on to which HD 229196 is seen projected and which we estimate to be approximately 18 arcmin in diameter (a dashed line outlines the approximate west boundary of this region). Since HD 229196 and G78.2+2.1 have comparable distances, it is possible that the ragged and apparently distorted appearance of the east side of the SNR results from an interaction between the stellar

wind of HD 229196 and the expanding shock wave of the SNR. There is fairly good agreement between the radio and IR structures, especially in the south–south-east and north. A comparison of the IR and optical images shows that the moderately bright IR emission barely 3 arcmin to the west–south-west of HD 229196 (there is also some weak corresponding radio continuum emission) is possibly a cloud of mixed gas and dust ionized and heated by the star, as is seen around WR 101 (Cappa et al. 2002a).

3.2 Neutral Hydrogen

The CGPS observations cover a velocity range between +58 and −152 km s^{-1} (all H I velocities are with respect to the local standard of rest – LSR). Fig. 4 (bottom) shows the average H I spectrum in a circular area of diameter 100 arcmin around the position of HD 229196. The most notable features are the local arm (from about +20 to −20 km s^{-1}), the Perseus arm (from −20 to −50 km s^{-1}), and the outer arm (from −50 to −120 km s^{-1}). Fig. 4 (top) shows the Galactic rotation curve along the line of sight to the star, required to transform an LSR velocity into a distance. The empirical curve of Brand & Blitz (1993) for three different longitudes as well as the theoretical relation for a flat rotation curve, with a circular velocity of 220 km s^{-1} at a Solar Galactocentric distance of 8.5 kpc, are presented. It is clear from this figure that, in addition to the inherent spatial confusion due to the fact that we are looking basically along a spiral arm, velocity crowding can be extremely severe especially for distances less than about 4 kpc.

Although the major radio structure in (or near) the field studied here is the SNR G78.2+2.1, previously studied in atomic hydrogen line emission by Landecker et al. (1980), our main purpose in this investigation is to find evidence for the interaction of HD 229196 with its surrounding ISM. In an ideal case, this would take the form of a deficiency of H I emission coincident with the stellar position and possibly of an excess of H I emission in a surrounding shell. In either case, in order to be significant, this deficiency should be visible over many km s^{-1}, as Arnal (1992) has shown that one can expect naturally occurring ('statistical') H I voids over small velocity ranges (typically less than about 8 km s^{-1}).

Assuming a distance of 1.3 kpc for HD 229196 and the velocity-distance relation shown in Fig. 4 (top), any H I structure at the same distance as the star would be expected to have an LSR velocity of 10 to 15 km s^{-1} (from the empirical curves) unless the stellar wind is impacting upon neutral gas whose velocity is affected by non-circular motions. Given the prominence of the nearby SNR G78.2+2.1 and the high level of activity in this region of the Galaxy (Lozinskaya 1992), this possibility cannot be ruled out.

Although all 256 individual H I channel images were inspected, for practical reasons, they are not reproduced in this paper. Instead, we first present the H I data averaged over six CGPS channels giving a velocity resolution of ~ 5 km s^{-1}. For ease of presentation, H I images have had a baseline subtracted equal to the average H I level in a 100-arcmin diameter central region in that velocity range. This does not distort the H I structure in the images, but simply reduces the dynamic range required for their display. The amount subtracted from each image can be read off the spectrum of Fig. 4 (bottom). Fig. 5 presents the resulting H I images for LSR velocities more positive than −12.5 km s^{-1} and where significant emission and features readily distinguishable from the general background can be seen. A fairly weak depression more or less centred on HD 229196 near 22 km s^{-1}, as well as a 'bay' or inflexion (at $l \approx 78°\,12'$, $b \approx 2°\,12'$) in a long and thick H I band or filament running
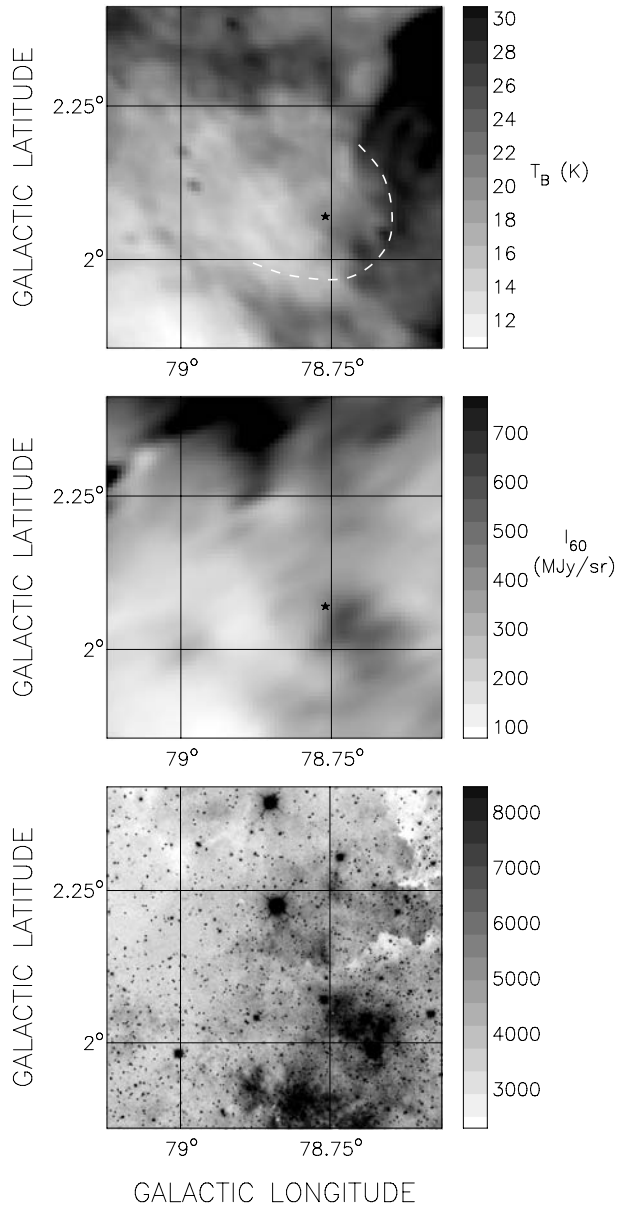

Figure 3. An enlarged view (outlined by the dashed-line box on the previous figures) of the immediate environs of HD 229196. Top panel: CGPS 1420-MHz continuum emission. The dashed line roughly outlines the SW boundary of the cavity. Middle panel: HIRES 60-μm continuum emission. Bottom panel: Reproduction of the optical emission in red from the digitized sky survey, in relative units.

diagonally through $l \sim 78°$, $b \sim 2°$ can be seen. This diagonal structure is interpreted by Landecker et al. (1980) as part of a slab of material accelerated by the SNR and we shall hereinafter refer to it as the 'slab'. Both the 'bay' and the 'slab' are indicated in Fig. 5.

In Fig. 6 we show a series of two-channel averages where the H I depression can be traced from about 27 to 17 km s^{-1}. The 'bay' is most noticeable at 22 and 20 km s^{-1}. Note that the apparent H I depression visible on the last image at ~ 14 km s^{-1} does not correspond to a true deficiency of H I but is an absorption artefact due to the intense radio continuum emission from G78.2+2.1 at this position (Landecker et al. 1980; Ladouceur & Pineault, in preparation).

To better circumscribe the H I depression associated with HD 229196, we averaged all channel images between about 27 and
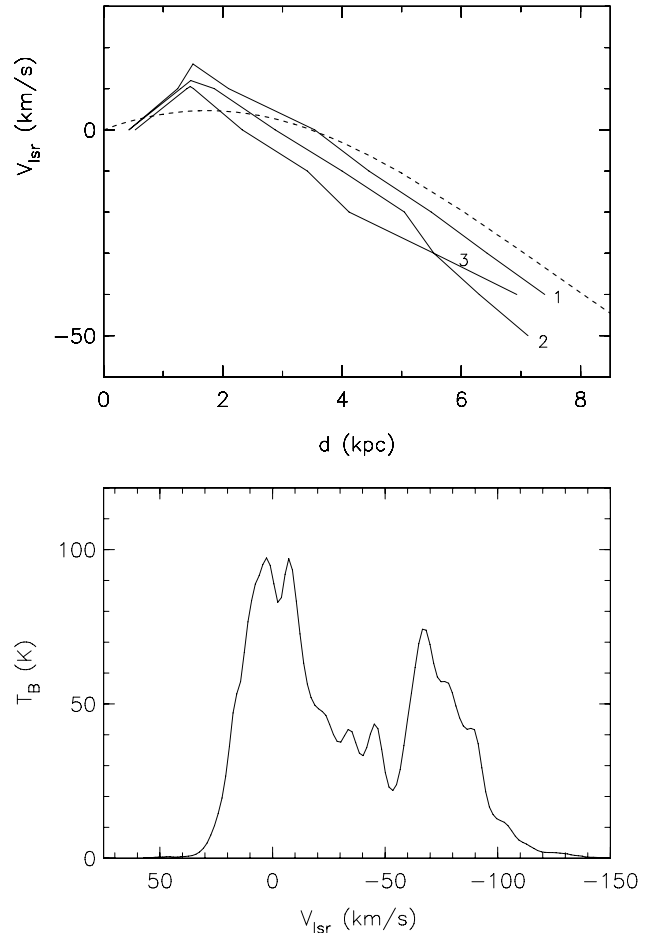

Figure 4. Top: Variation of kinematic distance as a function of velocity with respect to the LSR. The dashed line represents a flat rotation curve model with $R_0 = 8.5$ kpc and $v_0 = 220$ km s^{-1}, for the Galactic longitude of HD 229196. Solid lines are taken from Brand & Blitz (1993) and correspond to longitudes of (1) 77°.5, (2) 80° and (3) 82°.5. Bottom: average H I spectrum over a region of diameter 100 arcmin centred on the star.

20 km s^{-1}. The result is shown in Fig. 7. We are confident that the depression on to which HD 229196 is seen projected is real and significant. It is by no means regular, yet it correlates fairly well with the reduced continuum emissivity described previously. However, it appears significantly more extended and there is clearly no substantial evidence of a shell-like structure, the H I cavity being rather open towards the north and south.

4 ANALYSIS

In this section, we use the available data to determine the physical parameters of extended emission features possibly associated with HD 229196. As a consequence of the location of the star towards the Cygnus region of the Galaxy, foreground and background emission is important and renders an accurate determination of many parameters a somewhat difficult exercise.

Since HD 229196 appears so close in projection to the SNR G78.2+2.1 (although there is no a priori reason to expect that they are at the same distance or connected in any manner), it is useful to review the previous findings and conclusions of Landecker et al. (1980) in connection with their 21-cm H I observations. These authors propose a model in which the SNR progenitor exploded in a
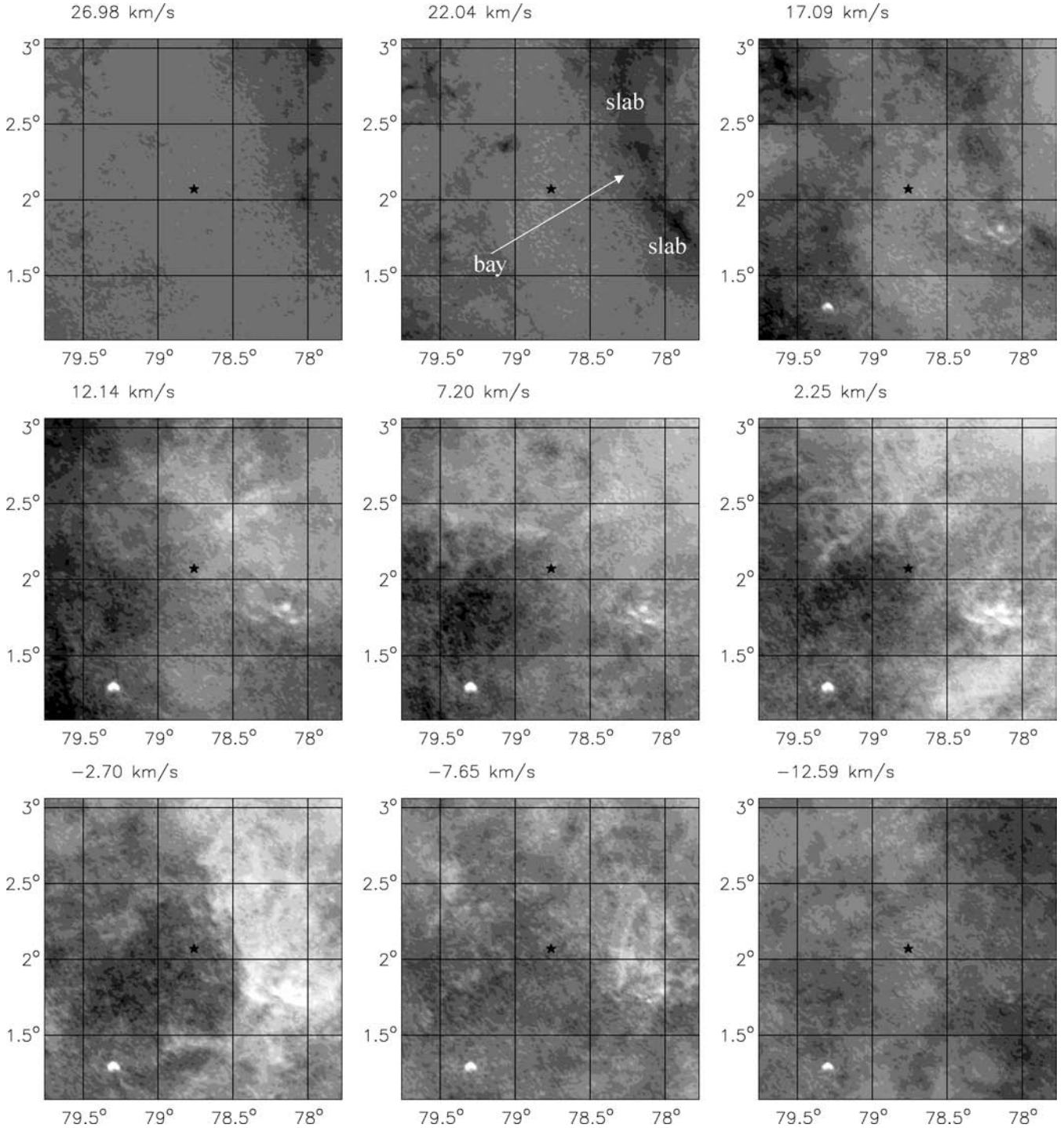
Figure 5. H I emission in the field centred on HD 229196, each image being an average over a velocity range of 5 km s^{-1}. The central LSR velocity of each image is indicated by the number at its top left-hand corner. Angular resolution is 2 arcmin. Grey-scale transitions are from −60 to +30 K in steps of 9 K relative to the average brightness temperature in the field at each velocity [shown in Fig. 4 (bottom)].

slab of material whose LSR velocity is approximately −5 km s^{-1} (the SNR systemic velocity). This eventually produced an H I shell having a current expansion velocity of about 25 km s^{-1}. The diagonal H I emission band at ∼22 km s^{-1} (labelled 'slab' in Fig. 5 and also seen over many channels in Fig. 6) is associated with the receding (far side) part of this shell. In their model, the brightest radio continuum features occur where the slab and expanding blast wave intersect. The SNR's distance is taken to be 1.5 kpc.

4.1 Standard interstellar bubble scenario

The 1420-MHz continuum image and average H I emission shown in Figs 1 and 7 are consistent with one another and with the notion that the continuum and H I cavities are caused by the star. However, the H I depression is quite shallow and significantly larger than its continuum counterpart, and the surrounding H I structure very incomplete. This is far from the canonical picture of a low-density
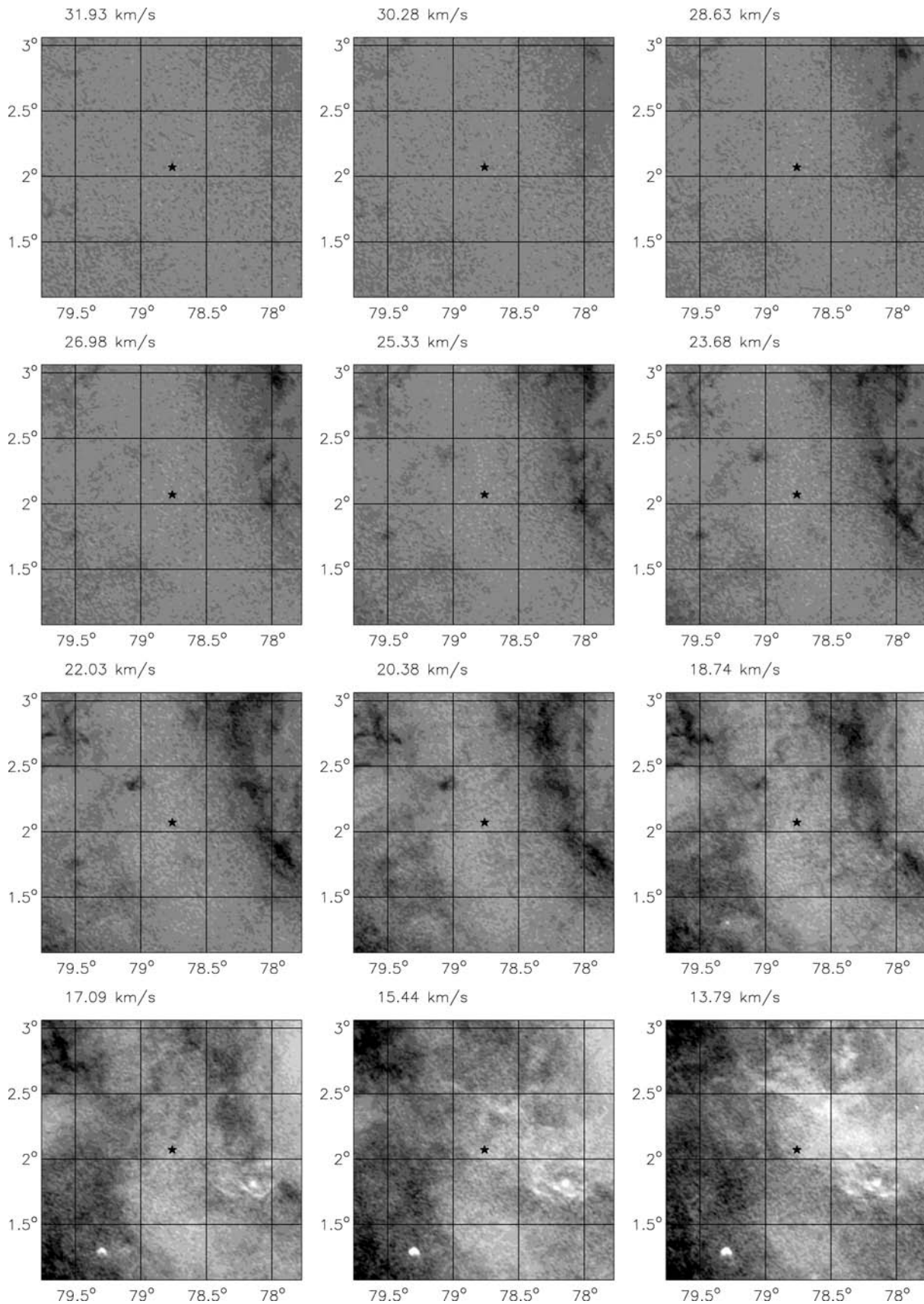
Figure 6. Same as Fig. 5 but with velocity resolution of 1.65 km s^{-1}. Angular resolution is 2 arcmin. Grey-scale transitions are from -40 to $+30$ K in steps of 7 K relative to the average brightness temperature in the field.
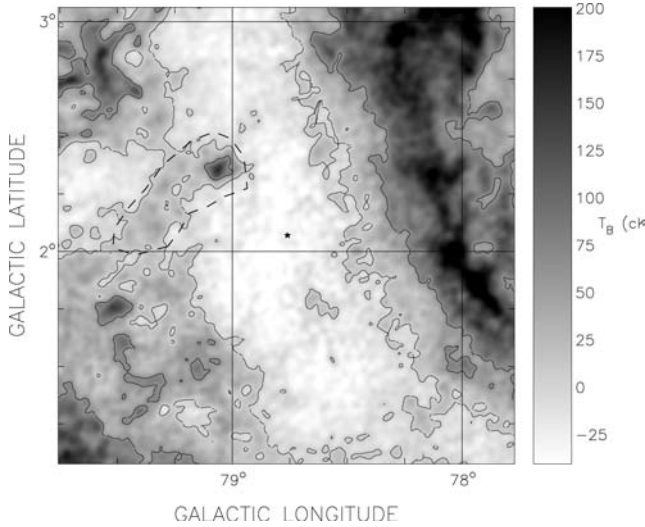
Figure 7. H I emission in the field centred on HD 229196 smoothed to 2 arcmin and averaged over the velocity range from about 27 to 20 km s^{-1}. Shadings run smoothly from −4 to +20 K relative to the average brightness temperature (∼12.4 K) in the field (note that the scale of the colour bar is in cK). Contours are at 0.4 and 6.4 K. The dashed polygon delimits an area used to estimate an H I mass (see text).

stellar wind bubble surrounded by a dense expanding shell (Castor et al. 1975; Weaver et al. 1977). In fact, except for an H I arc seen most obviously to the east (outlined by a dashed line in Fig. 7), it looks like very little material can be identified as having been swept up by the star's wind. Had any H I gas been acted upon by the stellar wind, it is unlikely to have formed a pressurized bubble around the star since the local ISM seems to be open in both the north and the south. Any expansion of the gas could then only be due to the transfer of wind momentum.

It is possible that the star has a much lower mass-loss rate than the value obtained by Lamers & Leitherer (1993). In a recent determination of the mass-loss rate of 40 Galactic O-type stars obtained by fitting stellar wind profiles to the P V resonance doublet lines, Fullerton, Massa & Prinja (2006) have shown that the determined mass-loss rates are systematically smaller than the ones obtained from Hα emission profile or radio free–free emission, by a median factor of ∼20, for stellar types between O4 and O7. They argued that these discordant measurements can be reconciled if the winds are strongly clumped on small spatial scales. Although HD 229196 is not part of the studied sample, another star of similar spectral type (HD 190864) showed a discrepancy by a factor of 20 in mass-loss rate. Note though that this factor of 20 translates into a factor of only $(20)^{1/5} \approx 1.8$ for the predicted radius and expansion velocity of the interstellar bubble in the energy-conservation phase (Lozinskaya 1992).

Regardless of the exact mass-loss rate, since there is no clear evidence of an H I shell structure surrounding HD 229196, it is not possible to unambiguously determine the mass of surrounding ISM material possibly affected by the star's wind.

As for the *bay* seen in the H I slab west of HD 229196, most evident on the 20 km s^{-1} image of Fig. 6, it could be interpreted as caused by the stellar wind impinging upon it. However, this H I feature is at a considerable distance (some 24 arcmin) outside the inner western edge of the continuum cavity around HD 229196, making the association uncertain. Furthermore the bay is seen, in projection, nearly in the middle of the SNR G78.2+2.1 outline (Fig. 1).

Landecker et al. (1980) have argued that the slab could be physically associated with the SNR and located on the far side of it with respect to us. Given these facts, the bay is not considered further in this work as we feel it is highly unlikely associated with HD 229196.

4.2 A bow shock scenario

The observed heliocentric radial velocity of −38 ± 5 km s^{-1} (Wilson 1953) of HD 229196 suggests that the space velocity of the star should be considered in a discussion of its effect on the surrounding ISM. The measured proper motion of the star, given in equatorial coordinates in Table 1, are first converted to proper motions in Galactic longitude and latitude, giving $\mu_\ell = -5.9 \pm 1.0$ mas yr^{-1} and $\mu_b = -1.5 \pm 1.0$ mas yr^{-1} for the Tycho-2 measurements, and $\mu_\ell = -6.3 \pm 0.75$ mas yr^{-1} and $\mu_b = 1.1 \pm 0.74$ mas yr^{-1} for the *Hipparcos* ones. The resulting proper motion vector is of limited interest since it gives the stellar motion with respect to the Sun. Of more interest is the *peculiar* speed (the absolute value of the peculiar velocity) $v_{\rm pec}$ of the star (i.e. its speed with respect to its local ISM). We follow the procedure described by van der Sluys & Lamers (2003) (after correcting the sign of the $w_\odot$ term in the last of their equation 19) and obtain

$$v_{{\rm pec},r} = -29.4 \pm 6.2 \ {\rm km \, s}^{-1},$$
$$v_{{\rm pec},l} = -10.3 \pm 10.0 \ {\rm km \, s}^{-1},$$
$$v_{{\rm pec},b} = -9.6 \pm 6.8 \ {\rm km \, s}^{-1},$$
$$v_{\rm pec} = 32.6 \pm 6.7 \ {\rm km \, s}^{-1},$$

when using the Tycho-2 proper motions, and

$$v_{{\rm pec},l} = -12.0 \pm 9.3 \ {\rm km \, s}^{-1},$$
$$v_{{\rm pec},b} = 6.8 \pm 5.4 \ {\rm km \, s}^{-1},$$
$$v_{\rm pec} = 32.5 \pm 6.7 \ {\rm km \, s}^{-1},$$

with the *Hipparcos* values ($v_{{\rm pec},r}$ is unchanged). The subscripts (r, l, b) denote radial, longitudinal and latitudinal components, respectively. In either case, the total peculiar speed is nearly 33 km s^{-1}, implying that the star is moving supersonically through its local ISM (unless the ISM temperature exceeds ∼90 000 K). Note that the l and b velocities have large errors. The major part of the peculiar motion of HD 229196 is nevertheless an approaching radial peculiar velocity corresponding to an inclination angle i with respect to the line of sight of about 25° ± 3°.

The corresponding tangential component of the peculiar velocity $v_{{\rm pec},t} = (v_{{\rm pec},l}^2 + v_{{\rm pec},b}^2)^{1/2}$ is essentially identical in magnitude for both sets of proper motions, namely 14 ± 8.5 km s^{-1}, which would, over a period of (say) 10^6 yr correspond to a relative displacement of the star with respect to its local ISM of 14 ± 8.5 pc or, an angular displacement of 37 ± 23 arcmin for a distance of 1.3 kpc. The typical lifetime of an Of star being 3×10^6 yr (Lozinskaya 1992), if HD 229196 is currently near the end of its Of phase, the relative displacement over this time could range anywhere from 42 arcmin to 3° (taking into account all possible combinations allowed by the errors on the longitude and latitude proper motions).

The supersonic motion of HD 229196 with respect to its local ISM should result in the formation of a bow shock structure aligned with the direction of motion of the star. Many such structures have been predicted and found around fast-moving stars (van Buren & McCray 1988; van Buren et al. 1990; van Buren, Noriega-Crespo & Dgani 1995; van der Sluys & Lamers 2003). We model the bow shock structure following Wilkin (1996) and assume a uniform medium of density ρ, and an isotropic stellar wind with mass-loss rate $\dot{M}$ and constant speed v_∞. The resulting structure has a paraboloidal
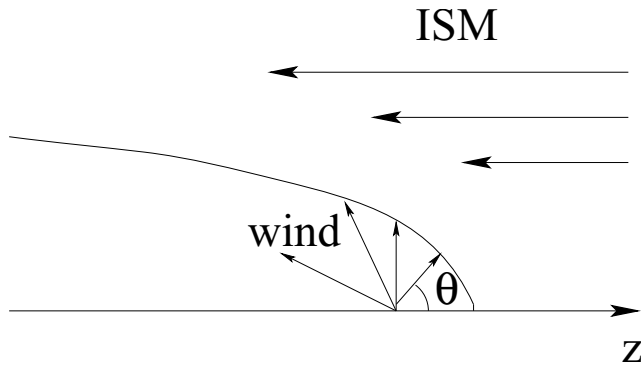
Figure 8. Graphical representation of the geometry of the bow shock model. The horizontal axis (z) represents the symmetry axis of the bow shock.

shape $R(\theta)$, with the stellar velocity vector as symmetry axis, given by

$$R(\theta) = R_0 \csc \theta \sqrt{3 (1 - \theta \cot \theta)}, \tag{1}$$

where θ is the polar angle from the axis of symmetry, as seen by the star at the coordinate origin (see Fig. 8), and R_0, the distance from the star to the point where the stellar wind and the ambient medium collide head-on ($\theta = 0$), is given by

$$R_0 = \sqrt{\frac{\dot{M} v_\infty}{4 \pi \rho v_{\rm pec}^2}}. \tag{2}$$

This standoff distance sets the length-scale of the bow shock.

Using a mass-loss rate $\dot{M} = 2 \times 10^{-6} \, {\rm M_\odot \, yr^{-1}}$, terminal velocity $v_\infty = 2500 \, {\rm km \, s^{-1}}$ and total peculiar speed of 32.5 km s^{-1}, we obtain $R_0 = 4.1 n_0^{-1/2}$ pc, where n_0, the number density, is in cm^{-3}. Using the components of the peculiar velocity, we deduce a corresponding projected distance of $1.7 n_0^{-1/2}$ pc which, at a distance of 1.3 kpc, gives an angular separation of $4.6 n_0^{-1/2}$ arcmin between the star and stellar wind cavity. From Fig. 3 (top), a crude fit to the radio continuum image gives an angular offset of ~ 5.3 arcmin between the star and the edge of the stellar wind cavity (roughly outlined by a dashed line), implying $n_0 \sim 0.75$ cm^{-3}, in agreement with generally accepted values of the ISM density.

This value of number density is however drastically changed if the mass-loss rate $\dot{M}$ has been overestimated by as much as a factor of ~ 20 (Fullerton et al. 2006). In this case, the deduced standoff distance R_0 would have to be decreased by a factor of $\sqrt{20} \approx 4.5$. Since, as shown by the above argument, the corresponding inferred number density n_0 is proportional to $\dot{M}$, the angular offset of ~ 5.3 arcmin would now imply a considerably lower value of $n_0 \approx 0.04$ cm^{-3}. Given the proximity of HD 229196 to the SNR G78.2+2.1, a possibility is that the star is travelling in a lower density ISM previously, but not totally, evacuated by the SNR progenitor.

In Fig. 9, we have drawn the peculiar proper motion direction vectors corresponding to both *Hipparcos* and Tycho-2 nominal values together with their respective 1σ deviations. The length of the arrows is arbitrary (it corresponds to the relative displacement of HD 229196 over a period of 3×10^5 yr for a peculiar velocity of 15 km s^{-1} and a distance of 1.3 kpc). It can be seen that the tangential peculiar motion of the star is essentially towards decreasing l values with a possibly large deviation above or below this direction. From the radial and tangential peculiar velocities, we can estimate the orientation of the paraboloidal bow shock cone with respect to the local ISM (details in van der Sluys & Lamers 2003). Insets in Fig. 9 show the appearance corresponding to both *Hipparcos* and
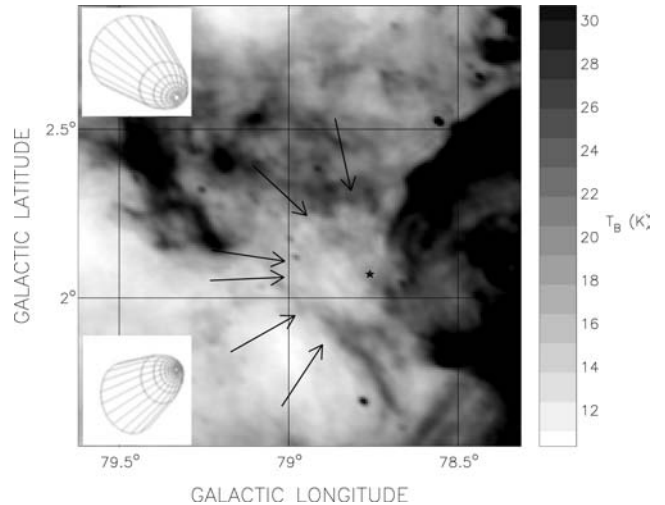
Figure 9. Radio continuum image indicating the possible incoming paths of HD 229196 according to *Hipparcos* (bottom three arrows) and Tycho-2 (top three). The length of the arrows is arbitrary. Insets show the bow shock structure orientation as it would appear (see text).

Tycho-2 nominal values. Although no attempt was made at a detailed fitting to the data and the sizes of the cones in the insets are arbitrary, it can be reasonably argued that the radio continuum data are consistent with, but do not require, a bow shock structure.

As for the observable part of the bow shock, it is important to keep in mind that the morphology depicted in Fig. 8 and the insets of Fig. 9 results from a number of simplifying assumptions and that one should really use it only as a guide. Numerical simulations of bow shocks (e.g. Mac Low et al. 1991; Raga et al. 1997; Arthur & Hoare 2006) have shown that, whereas the simple Wilkin model traces relatively well the average position of the bow shock, it underestimates the standoff distance by a factor of about 1.5, as was already predicted by van Buren & McCray (1988). Using this larger value for R_0 would cause the ambient density estimate to be decreased by a factor of 1.22, from 0.75 to 0.61 cm^{-3}.

Concerning the extent of the visible part of the bow shock, Mac Low et al. (1991) visualized their numerical model by calculating the free–free continuum radiation along rays through the shell, thus obtaining images of the predicted intensity for a number of different viewing angles i. Although their standard model is for a star moving relatively slowly into a dense molecular cloud, the shapes are self-similar and their images provide a reliable indication of the relative brightness across the structure. The figure from Mac Low et al. (1991) corresponding to our deduced inclination angle of about 25° (their fig. 5) shows that the emission is concentrated in the forward hemisphere, the relative brightness quickly decreasing away from the apex of the bow shock and becoming negligible for $\theta \geqslant 125°$ (Fig. 8).

5 DISCUSSION

The line of sight towards HD 229196 is along a spiral arm and includes regions where there is evidence of intense activity generating significant non-circular motions (Lozinskaya 1992). The presence of the bright SNR G78.2+2.1 next to HD 229196 adds to the difficulty of identifying structures clearly related to the star. Nevertheless, the depressed radio continuum emission coincident with the star can credibly be attributed to the action of the stellar

wind and ionizing photons. Furthermore the relatively large peculiar velocity of the star cannot be ignored.

The actual appearance of the structure created by a fast moving star possessing a strong stellar wind not only depends critically on the velocity and inclination angle with respect to the line of sight, but also on the time over which the stellar wind has been acting on the surrounding ISM. This particular context was briefly addressed by Weaver et al. (1977) who defined a critical time t_c allowing one to roughly classify the expected morphology,

$$t_c = 2 \times 10^6 \, n_0^{-1/2} L_{36} (v_{pec}/20 \, \text{km s}^{-1})^{-5/2} \, \text{yr}, \tag{3}$$

where L_{36} is the wind luminosity in units of $10^{36} \, \text{erg s}^{-1}$. For $t \ll t_c$, there is hardly any departure from the standard ISM bubble scenario (e.g. Castor et al. 1975), whereas for $t \gg t_c$ the structure bears essentially no resemblance to it (except for zero inclination angle) but is instead accurately described by the bow shock paraboloidal structure shown in Fig. 8. Using the parameter values appropriate for HD 229196 in its Of phase, we obtain $t_c \sim 10^6 n_0^{-1/2}$ yr. Considering that the Of phase of HD 229196 has most certainly been preceded by the wind-losing phase of a standard OB star (a possible total duration of 3×10^6 yr), it is likely that the star is now observed at a stage where $t \gg t_c$ (corresponding to fig. 7c in Weaver et al. 1977). However, the fact that HD 229196 is encountering its local ISM at a relatively small inclination angle of about $25°$ with respect to the line of sight would tend to make any bow shock structure less obvious than that sketched on the last figure of Weaver et al. (1977). Finally, the extreme uncertainty in the proper motion (the *Hipparcos* and Tycho-2 values do not even agree within their nominal errors) makes it useless to attempt any modelling based on bow shock theory.

The situation with respect to the neutral gas is considerably more complicated. Although a slight depression in the H I distribution is present, this cannot be taken as firm evidence of a canonical inter-stellar bubble surrounded by an expanding H I shell. In the standard bubble scenario, this could be explained by the fact that the ISM is highly inhomogeneous, preventing the formation of a pressurized bubble. The wind momentum could still be transferred to adjacent gas though, leading to a distorted concave structure and this is possibly what is being seen in the east–south-east (Fig. 7).

We have seen however that the peculiar motion of the star is supersonic. The magnitude of this velocity is mostly due to its large radial velocity (Wilson 1953) and this should ideally be confirmed independently. Be that as it may, taking the measurements (with their quoted errors) at face value leads to the conclusion that a weak bow shock structure should have formed around HD 229196. This situation is strikingly different from the standard bubble case since an expanding H I shell does not form. The incoming matter is shocked, ionized and moves tangentially along the thin bow shock layer (i.e. along the cone shown in Fig. 8). It is far from clear whether the shocked matter can ever recombine to form a neutral H I layer and, if it does, where this occurs. It is likely to be significantly far downstream from the star, where the tangential velocity has become negligible. The primary H I signature of a bow shock is thus likely to be that of an elongated H I cavity having a conical structure aligned with the projected direction of motion of the star (i.e. the empty interior within the bow shock surface). Brown & Bomans (2005) have provided evidence that such an H I structure is present around the O6.5V star HD 17505 whose peculiar velocity they estimate as 25.7 km s^{-1}. If the ISM into which the star is travelling is inhomogeneous, the resulting bow shock structure is expected to be more irregular and may significantly depart from the paraboloidal shape depicted in Fig. 8.

A further prediction of the bow shock model is that shocked gas located at the apex of the bow shock should have the same velocity as the star (the bow shock is a stationary structure in the frame of the star). If dense enough, the shocked gas may trap the ionization front within the shell so that the outer part may remain neutral. Using the criterion given by Mac Low et al. (1991) and the parameters appropriate to HD 229196, we find that only half of the shell should be ionized. The neutral gas would thus be observed at an LSR velocity equal to the sum of the radial components of the systemic velocity of the local ISM and the stellar peculiar velocity which, in this case, would be in the range -8 to -25 km s^{-1}. As can be seen from Fig. 4 general Galactic H I emission is very strong in this range so that there is no hope of finding any signature of emission originating from near the bow shock apex. It might however be worthwhile to look for such a signature in more 'favourable' cases, such as where the velocity of the apex gas falls in a velocity range of negligible Galactic emission.

6 CONCLUSION

Given the high level of confusion along the line of sight to HD 229196, the interpretation of the H I data is far from easy. Although we have tentatively associated a shallow H I cavity with the star, HD 229196 seems another case of a star where there is no unambiguous evidence of the interaction of the star with its surrounding neutral material although, on the basis of its spectral type alone, one would certainly expect to see signs of interaction. There are indications that the ISM is inhomogeneous, preventing the formation of a pressurized structure. It is also possible that the mass-loss rate of the star may have been severely overestimated. Furthermore the supersonic velocity of the star with respect to its local ISM implies the absence of a classical expanding H I shell.

The 1420-MHz CGPS continuum radio image shows the star projected within a region of depressed emission consistent with the clearing action of the star's wind and ionizing luminosity. The shape and orientation of this radio structure is in general agreement with a weak bow shock arising from the supersonic motion of the star, although it could also be due entirely or partly to a density gradient in the surrounding ISM. It is possible that a distortion in the east side of the SNR G78.2+2.1 is the result of an interaction between the stellar wind of HD 229196 and the expanding SNR shock wave.

The fact that HD 229196, an Of-type star member of a class of particularly strong stellar wind emitters, does not seem to affect its environments in a spectacularly striking manner, is a further indication of the need for a systematic approach. It also underlines the importance of using uniform and homogenous data bases, such as the CGPS, which minimize selection effects and provide large-area coverage, and of avoiding preconceived ideas about what to expect for the morphology of the ISM around massive stars. Such a systematic study should make it possible to better disentangle the relative effects of an inhomogeneous surrounding ISM and of a non-negligible stellar velocity. The current study has emphasized the need to select targets which keep confusion effects to a minimum.

REFERENCES

Arnal E. M., 1992, A&A, 254, 305
Arthur S. J., Hoare M. G., 2006, ApJS, 165, 283
Avedisova V., 1972, SvA, 15, 708
Bieging J. H., Abbott D. C., Churchwell E. B., 1989, ApJ, 340, 518
Brand J., Blitz L., 1993, A&A, 295, 67
Brown D., Bomans D. J., 2005, A&A, 439, 183
Cappa C. E., Herbstmeier U., 2000, AJ, 120, 1963
Cappa C. E., Dubner G., Rogers C., St-Louis N., 1996, AJ, 112, 1104
Cappa C. E., Goss W. M., Pineault S., 2002a, AJ, 123, 3348
Cappa C., Pineault S., Arnal E. M., Cichowolski S., 2002b, A&A, 395, 955
Cappa C. E., Arnal E. M., Cichowolski S., Goss W. M., Pineault S., 2003, in van der Hucht K. A., Herrero A., Esteban C., eds, Proc. IAU Symp. 212, A Massive Star Odyssey: From Main Sequence to Supernova. Astron. Soc. Pac., San Francisco, p. 596
Cappa C., Goss W. M., van der Hucht K. A., 2004, AJ, 127, 288
Cao Y., Terebey S., Prince T. A., Beichman C. A., 1997, ApJS, 111, 387
Castor J., McCray R., Weaver R., 1975, ApJ, 200, L107
Cazzolato F., Pineault S., 2000, AJ, 120, 3192
Chu Y.-H., Treffers R. R., Kwitter K. B., 1983, ApJS, 53, 937
Cichowolski S., Arnal E. M., 2004, A&A, 414, 203
Cichowolski S., Pineault S., Arnal E. M., Testori J. C., Goss W. M., Cappa C. E., 2001, AJ, 122, 1938
Cichowolski S., Arnal E. M., Cappa C. E., Pineault S., St-Louis N., 2003, MNRAS, 343, 48
Cichowolski S., Pineault S., Arnal E. M., Cappa C. E., 2008, A&A, 478, 443

Fowler J. W., Aumann H. H., 1994, in Terebey S., Mazzarella J., eds, Science with High-Resolution Far-Infrared Data. Jet Propulsion Laboratory, Pasadena, p. 1
Fullerton A. W., Massa D. L., Prinja R. K., 2006, ApJ, 637, 1025
Garmany C. D., Stencel R. E., 1992, A&AS, 94, 211
Higgs L. A., Tapping K. F., 2000, AJ, 120, 2471
Howarth I. D., Prinja R. K., 1989, ApJS, 69, 527
Lamers H. J. G. L. M., Leitherer C., 1993, ApJ, 412, 771
Landecker T. L., Roger R. S., Higgs L. A., 1980, A&AS, 39, 133
Landecker T. L. et al., 2000, A&AS, 145, 509
Lozinskaya T. A., 1982, Ap&SS, 87, 313
Lozinskaya T. A., 1992, Supernovae and Stellar Wind in the Interstellar Medium. Am. Inst. Phys., New York
Mac Low M.-M., van Buren D., Wood D. O. S., Churchwell E., 1991, ApJ, 369, 395
Maíz-Apellániz J., Walborn N. R., Galué H. A., Wei L. H., 2004, AJS, 151, 103
Marston A. P., 1996, AJ, 112, 2828
Pineault S., 1998, AJ, 115, 2483
Raga A. C., Noriega-Crespo A., Cantó J., Steffen W., van Buren D., Mellema G., Lundqvist P., 1997, Rev. Mex. Astron. Astrophys. 33, 73
Reich W., Reich P., Fürst E., 1997, A&AS, 126, 413
Schmidt-Kaler Th., 1982, Bull. Inf. Cent. Donnees Stellaires, 23, 2
Taylor A. R. et al., 2003, AJ, 125, 3145
Vacca W. D., Garmany C. D., Shull J. M., 1996, ApJ, 460, 914
van Buren D., McCray R., 1988, ApJ, 329, L93
van Buren D., Mac Low M.-M., Wood D. O. S., Churchwell E., 1990, ApJ, 353, 570
van Buren D., Noriega-Crespo A., Dgani R., 1995, AJ, 110, 2914
van der Sluys M. V., Lamers H. J. G. L. M., 2003, A&A, 398, 181
Walborn N. R., 1971, ApJS, 23, 257
Walborn N. R., 1973, AJ, 78, 1067
Weaver R., McCray R., Castor J., Shapiro P., Moore R., 1977, ApJ, 218, 377
Wilkin F. P., 1996, ApJ, 459, L31
Willis A. G., 1999, A&AS, 136, 603
Wilson R. E., 1953, General Catalog of Radial Velocities Carnegie Institution Publication No. 601, Washington
Zhang X., Zheng Y., Landecker T. L., Higgs L. A., 1997, A&A, 324, 641

This paper has been typeset from a TeX/LaTeX file prepared by the author.